

Light Emission from Graphite Surfaces during Beam Bombardment, Observation and Consequences for use of Graphite in Divertors

D Ciric, H D Falter, P Massmann, K N Mellon.

JET Joint Undertaking, Abingdon, Oxon, OX14 3EA, UK.

"This document is intended for publication in the open literature. It is made available on the understanding that it may not be further circulated and extracts may not be published prior to publication of the original, without the consent of the Publications Officer, JET Joint Undertaking, Abingdon, Oxon, OX14 3EA, UK".

"Enquiries about Copyright and reproduction should be addressed to the Publications Officer, JET Joint Undertaking, Abingdon, Oxon, OX14 3EA".

A substantial amount of visible and infrared light is emitted from the target surface during the bombardment of graphite and carbon fibre composite targets by high power particle beams. The emission is caused by the presence of a micron size carbon particles loosely bound to the target surface which reach the radiation equilibrium with the incoming beam within milliseconds. The carbon particle coverage can be reduced by extensive high power beam ($\geq 15 \text{ MW/m}^2$) bombardment and can be correlated with methane release from carbon targets. These observations have important consequences for the use of such materials for plasma facing components in, e.g., divertors.

1. INTRODUCTION

During the design phase of the JET MkII divertor [1] tests of a large number of graphite samples from many different manufacturers have been carried out at JET Neutral Beam Test Bed. These tests show that a substantial amount of visible and infrared light is emitted from the tile surface during the bombardment of the tile by hydrogen and helium beams with power densities ranging between 5 and 30 MW/m^2 . The effect was observed on both actively cooled and inertial tiles made of various Carbon Fibre Composite (CFC) materials.

A quantitative explanation for the observation made under all experimental conditions has been developed by assuming the presence of small particles (micron size) which are loosely bound to the target surface. These rapidly achieve radiation equilibrium with the incident power density. Consequently, particles heat up to high temperatures where sublimation rates are not negligible.

2. EXPERIMENT

CFC tiles are placed at the beam centre line of the JET Neutral Beam Test Bed at a distance of 7 metres from the beam source (Figure 1). Tiles are exposed to particle beams with peak power densities ranging between 5 and 30 MW/m^2 , with a pulse duration between 0.5 and 10 seconds. Beam power density distribution along two lines perpendicular to

the beam axis is measured by an array of inertial copper blocks (inertial calorimeter).

The CFC target surface temperature distribution is measured by an AGEMA Thermovision 900 SW infrared imaging system. Infrared (IR) images are recorded at a rate of 15 Hz. One-dimensional line images are recorded at faster rates - up to 2.55 kHz. The IR imaging system has a temperature range 0 - 2000°C and the accuracy of 1%. Several thermocouples are used to monitor the CFC target bulk temperature. The emissivity of the target is determined from the comparison between IR and thermocouple signals when the target is heated up to a thermal equilibrium at several hundred °C.

Every beam pulse is recorded using two CCD video cameras. The methane release from the target during the beam pulse is monitored by measuring the corresponding gas flow rate with a residual gas analyser.

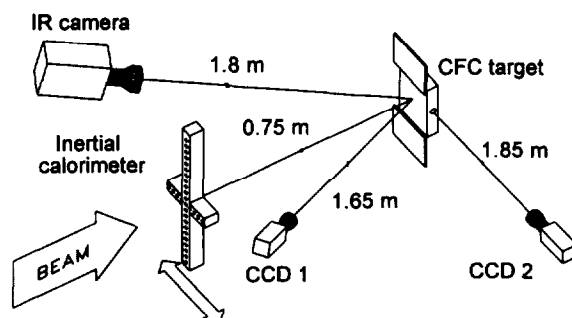


Figure 1: Layout of the experiment.

2. OBSERVATIONS

Intensive infrared light emission distorts the signal recorded by the thermal imaging system used to assess thermal properties of the CFC material. This is illustrated on Figures 2 and 3. Figure 2 shows two images of the Mitsubishi MFC-1 tile exposed to a 17 MW/m^2 hydrogen beam for 0.5 s. Only the second image, recorded after the beam pulse, reflects the true surface temperature of the CFC target. This is clearly visible from temperature distributions (Figure 3) derived from IR images shown in Figure 2. The temperature distribution in Figure 3.a shows "hot spots" attributed to the high temperature carbon particles. It should be noted that the target was machined by grinding and ultrasonically cleaned before the experiment. Images similar to those shown in Figure 2 were also recorded by video cameras.

A rapid step change in the surface temperature is observed when the beam is switched on or off. Figure 4 shows the fast time trace (0.39 ms resolution) of the Dunlop DMS-704 CFC target exposed to 30 MW/m^2 modulated hydrogen beam. The time constant of this step change in surface temperature is in the millisecond region. The "noise" present in the infrared signal during the beam on periods corresponds to the fluctuations in the power density caused by the variation of the beam current. This target was also machined by grinding but was not cleaned ultrasonically before the test.

Particle sizes in the range $1\text{-}10 \mu\text{m}$ can be inferred from the measured radiation characteristics in agreement with that observed for the size of particles which can be mechanically removed from the surface.

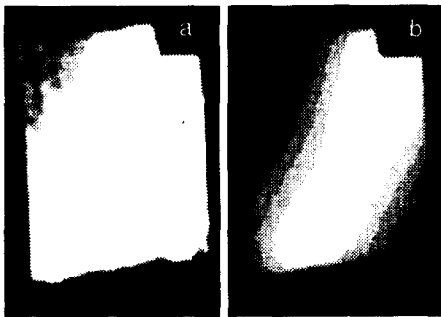


Figure 2: IR images of the Mitsubishi MFC-1 target exposed to 17 MW/m^2 Hydrogen beam for 0.5 s: a) end of pulse, b) 0.1 s after the end of pulse.

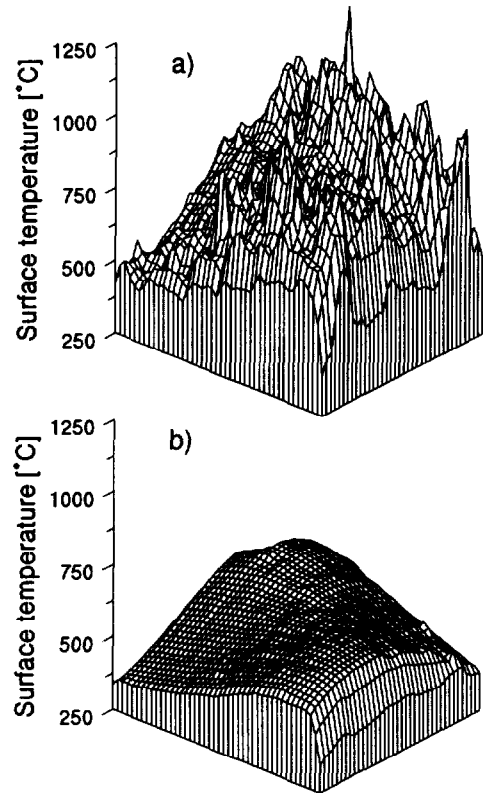


Figure 3: Temperature distributions of the MFC-1 target derived from IR images shown in Figure 2.

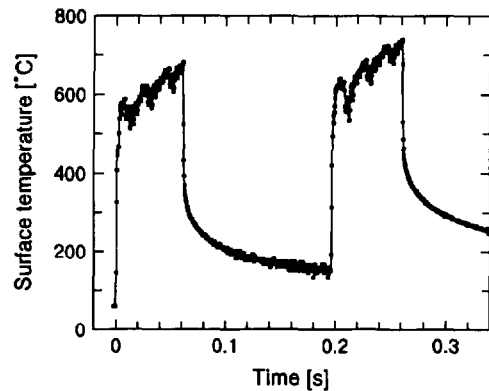


Figure 4. Surface temperature trace of the Dunlop DMS-704 target exposed to 30 MW/m^2 modulated Hydrogen beam.

Similar effects were observed for practically all CFC materials tested (more than 15 samples made by 5 different manufacturers). In some cases only isolated high temperature "islands" were observed, while for some materials the entire surface of the tile

was radiating at very high temperature during the beam pulse. The intensity of the radiation was much higher for targets which were not ultrasonically cleaned prior to the test. It was also observed that the amplitude of the temperature step increases with the beam power density.

3. MODEL

We assume that the radiation power density $W(T_M)$ measured by the IR imaging system is a linear combination of two signals: one representing the true surface temperature of the material - $W(T_B)$, and one representing the temperature of the carbon particles loosely bound to the CFC target - $W(T_p)$. The weighting function is the carbon particle coverage θ (≤ 1):

$$W(T_M) = \theta W(T_p) + (1 - \theta) W(T_B). \quad (1)$$

The radiation power density $W(T)$ is determined by the instrumental function of the IR imaging system which is:

$$W(T) = \frac{R}{\exp(B/T) - F}, \quad (2)$$

where R , B and F are calibration constants.

The temperature of the carbon particles (T_p) is determined from the radiation equilibrium condition:

$$p = f \sigma T_p^4, \quad (3)$$

where p is the beam power density, σ is the Stefan-Boltzman constant and f is the form factor determined by the ratio of the radiating and absorbing area of the particle. Form factor f (the only free parameter in the model) is determined by the shape and the orientation of the particle with respect to the incoming heat flux. For the particle of spherical shape the value of f is $4\pi r^2/\pi r^2 = 4$. For particles of irregular shapes one could expect values of $f \sim 10$. Figure 5 illustrates the influence of the form factor f on the particle temperature. The heat conduction from the high temperature particle to the target material is neglected in the model, but can be introduced by an increase in the value of f .

The surface temperature of the bulk material will initially follow the $t^{1/2}$ law:

$$T_B(t) - T_{B0} = p A \sqrt{t}, \quad (4)$$

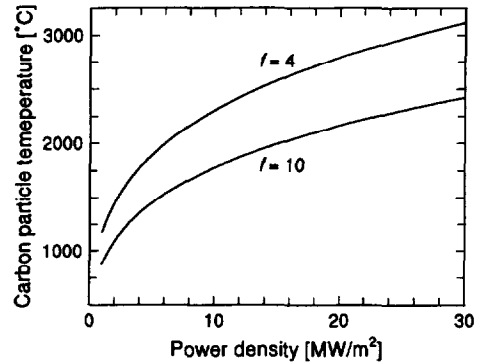


Figure 5. Carbon particle temperature determined from the radiation equilibrium condition.

where T_{B0} is the bulk surface temperature prior to the beam pulse, p is the beam power density, t is time and A is the parameter determined by thermal properties of the material.

The surface coverage θ and parameter A can be determined by the least square fit of the equation (1) to the IR camera signal - $W(T_M(t))$. Since thermal properties of CFC materials are temperature dependent, the parameter A also varies with temperature. To avoid this uncertainty, the fitting procedure should be restricted to a fixed temperature range (e.g. 300 - 1000°C), in which case the value of A remains constant. The typical result of the fitting procedure is shown in Figure 6.

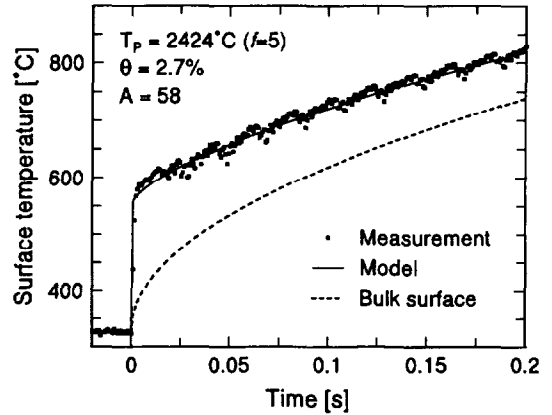


Figure 6. Initial surface temperature rise of the Dunlop DMS-704 target exposed to 15 MW/m² hydrogen beam.

4. RESULTS AND DISCUSSION

The amplitude of the step change in the surface temperature is the measure of the carbon particle

coverage. This temperature step was observed on all investigated targets. The surface particle coverage of up to 10% was deduced by applying the above described model with $f=5$. It should be noted that the particle coverage is dependent on the value of the form factor f . Nevertheless, by applying one fixed value of f , the relative change of the particle coverage during the test can be determined with reasonable accuracy.

It was established that the amplitude of the step, and hence the surface coverage, can be reduced by extended exposures of the target to high power ($\geq 15 \text{ MW/m}^2$) particle beams. In some experiments the methane release from the target during its exposure to the beam was measured. We found that the methane production can be correlated with the particle coverage (Figure 7).

For some of the tested samples the step change in the surface temperature was not observed in the initial stages of the experiment. For those targets the measured surface temperature follows the $t^{1/2}$ law (left diagram in Figure 8). However, after extended exposures to high power particle beams the reappearance of the temperature step corresponding to low particle coverage was found. Figure 8 shows time traces of the surface temperatures at the beginning and at the end of one such test. The Dunlop DMS-704 sample, which was machined by milling and ultrasonically cleaned before the test, was exposed to a sequence of 2 s long hydrogen beam pulses at 15 MW/m^2 . The result of the test was that the surface coverage was gradually increased during the course of the experiment to a saturation value of 0.8%.

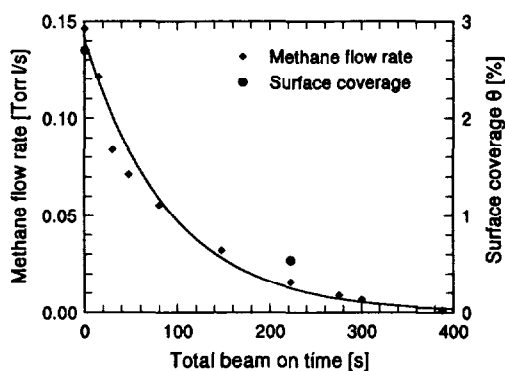


Figure 7. Methane release and carbon particle coverage during the endurance test of the Dunlop DMS-704 using 15 MW/m^2 hydrogen beam. The target was not cleaned ultrasonically prior to the test.

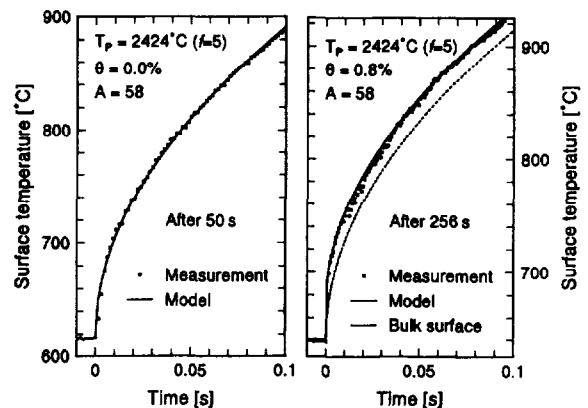


Figure 8. Temperature traces recorded during the endurance test of the Dunlop DMS-704 using 15 MW/m^2 hydrogen beam. The target was cleaned ultrasonically prior to the test.

Our findings can be summarised as follows:

- The presence of high temperature carbon particles loosely bound to the CFC material surface should be taken into account when interpreting IR thermometry data.
- The initial coverage of the surface by these particles can be shown to be $\leq 10\%$ and reduces to $\leq 1\%$ by extended exposure to the high power beam.
- Initially particle-free tiles develop a low coverage ($\leq 1\%$) after long exposures to high power beams.

These observations have important consequences for the use of CFC materials as plasma facing components. They suggest that, in terms of impurity production, the surface condition of the material could be at least as important as its bulk thermal properties. Although we have shown that the surfaces can be cleaned (conditioned) by extended exposure to high heat fluxes, this would translate into many tens or even hundreds of plasma discharges. Further work is required to assess the in situ wall cleaning or conditioning in terms of the removal of micron sized particles.

REFERENCE

1. H. Altmann *et al.*, "Design of the JET MkII Divertor with Large Carbon Reinforced Carbon CFC Tiles", These proceedings